Enzyme–Inhibitor Complexes

DOI: 10.1002/ange.200905597

Structural Basis of α-Fucosidase Inhibition by Iminocyclitols with K_i Values in the Micro- to Picomolar Range**

Hsing-Ju Wu, Ching-Wen Ho, Tzu-Ping Ko, Shinde D. Popat, Chun-Hung Lin, and Andrew H.-J. Wang**

Glycosidases[1] catalyze the hydrolysis of glycosidic bonds and are often therapeutic targets; examples include the influenza virus neuraminidase, which is targeted by Tamiflu,[2] and intestinal disaccharidases involved in type II diabetes.[1,3] Iminocyclitols (also called iminosugars or azasugars) represent an important glycosidase inhibitor class. Protonated at physiological pH to mimic the "oxocarbenium-ion-like" transition state, they usually offer satisfyingly high affinity toward glycosidases.[4] Some of these molecules have been characterized by structural and mechanistic methods to understand their interactions with enzyme active sites.[5] However, only limited information is available for the identification of important factors that contribute to high inhibition potency (lower than nanomolar K_i values) as well as to the dynamic motion of the glycosidase–inhibitor interaction transition from low to high binding affinity. α-Fucosidase is associated with many disorders including inflammation,[6] cancer,[7] cystic fibrosis,[8] and fucosidosis.[9] The enzyme is considered an early biomarker for detecting hepatocellular and colorectal carcinomas,[10] and is released by gastric epithelial cells only upon infection with *Helicobacter pylori* to affect the bacterial growth, adhesion, and pathogenicity.[11] Herein we report nine X-ray crystal structures of the *Thermotoga maritima* enzyme (TmF) in complex with iminocyclitols **1**–**9**, which have K_i values spanning the micro- to picomolar ranges and up to 10^6-fold variation in potency (Figure 1).[12] These inhibitors are C1- or C5-substituted fuconojirimycin (FNJ) derivatives. Compounds **2**–**6** show time-dependent, slow-binding inhibition events that undergo progressive tightening of the enzyme–inhibitor complex from a low-nanomolar K_i value to a picomolar K_i*.[13] Compound **2** is the most powerful glycosidase inhibitor known ($K_i^* = 0.47$ pM), whereas compound **9** is the least potent ($K_i = 6.0$ μM; Figure 1).

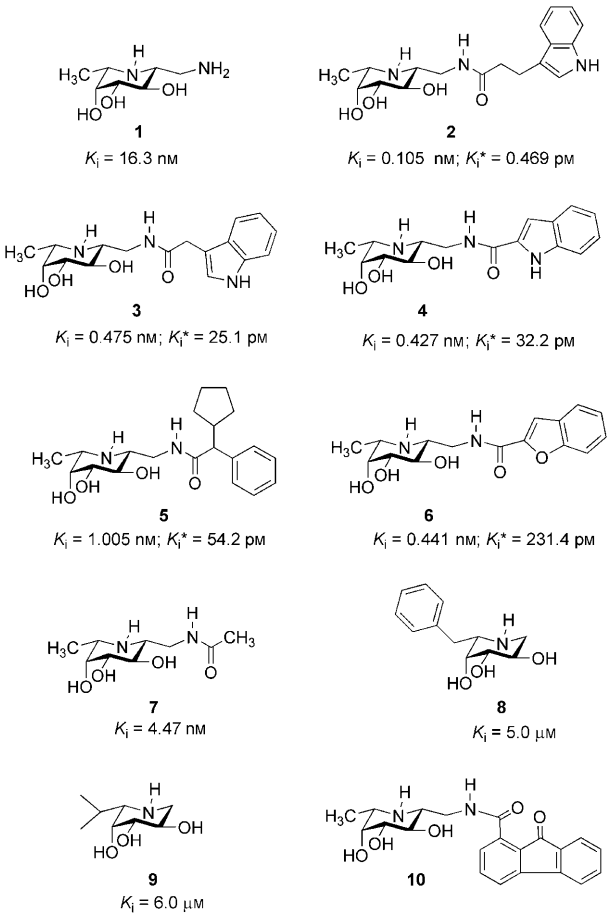

Figure 1. Structures of compounds **1**–**10** and their corresponding inhibition constants for TmF. The K_i of **10** for human α-fucosidase is 0.40 nM.

The overall assembly of TmF–inhibitor complexes in our crystals is similar to the previous TmF–fucose structure (PDB code: 1ODU[14]), with two trimers stacked on top of each other (Figure S1A in the Supporting Information). Parts of three surface loops, T47–M55 (loop 1), V269–G273 (loop 2), and G297–H300 (loop 3),[14] were previously obscured, but are clearly visible in our structures (Figure S1B in the Supporting Information). The TmF active site is located in a small pocket formed by the C-terminal ends of β strands of the central $(\beta/\alpha)_8$ barrel (Figure S1B in the Supporting Information). With the exception of **8** and **9**, all inhibitors

[*] Dr. H.-J. Wu, C.-W. Ho, Dr. T.-P. Ko, Dr. S. D. Popat, Prof. C.-H. Lin, Prof. A. H.-J. Wang
Institute of Biological Chemistry, CBMB, Taiwan International Graduate Program, Academia Sinica
128 Section 2, Academia Road, Nankang, Taipei 11529 (Taiwan)
Fax: (+886) 2-2788-9759
E-mail: chunhung@gate.sinica.edu.tw
ahjwang@gate.sinica.edu.tw
C.-W. Ho
Department of Chemistry, National Tsing-Hua University
Taipei (Taiwan)

[**] This work was supported by Academia Sinica and the National Science Council (95-3112-B-001-015). We thank NSRRC of Taiwan, SPring-8 of Japan, and ALS of USA for beam time allocations. H.-J. W. is grateful for an NHMRC C. J. Martin Fellowship from Australia.

Supporting information for this article is available on the WWW under http://dx.doi.org/10.1002/anie.200905597.

have an extra substituent at C1 (also called aglycon) residing at the β position. These inhibitors adopt a product-like $^{1}C_{4}$ (chair) conformation rather than the transition-state $^{3}H_{4}$ (half-chair) conformation.[15] In spite of the isopropyl group at C5, compound **9** binds in the same orientation as other compounds with a C1 substituent (Figure 2).

Comparison of the active sites among the nine structures indicates that the observed 10^{6}-fold difference in inhibition potency is the result of several major factors. For clarity, only three complex structures are detailed herein to represent the various levels of binding affinity: TmF–**1** ($K_i = 16$ nM), TmF–**2** ($K_i^* = 0.47$ pM), and TmF–**9** ($K_i = 6$ μM; Figure 2). Specific binding interactions for the other inhibitors are described in the Supporting Information and Figure S2. Most clearly, loops 1 (residues 46–65) and 2 (residues 266–275) are stabilized by binding to inhibitors that have higher affinity than that of fucose ($K_M = 50$ μM),[14] and are thus visible in all TmF–inhibitor complex structures presented herein. Depending on how they interact with the bound inhibitor, the two loops vary slightly in their conformation (Figure S3 in the Supporting Information). They are more open in the TmF–**9** complex than in TmF–**1**. The loops are indirectly associated in the TmF–**9** complex via adjacent water molecules (L and N) interacting with Y64 and E266. In contrast, the two loops in the TmF–**1** complex make direct contacts by forming hydrogen-bond pairs between E49–H268 (Figure S4 in the Supporting Information) and Y64–E266 (Figure 2), as well as the hydrophobic interaction between L50 and V269 (Figure S4 in the Supporting Information). The conformational differences mainly result from interactions between the inhibitor and the two catalytically important residues, namely E266 (the catalytic acid/base residing in loop 2) and D224 (the nucleophile).

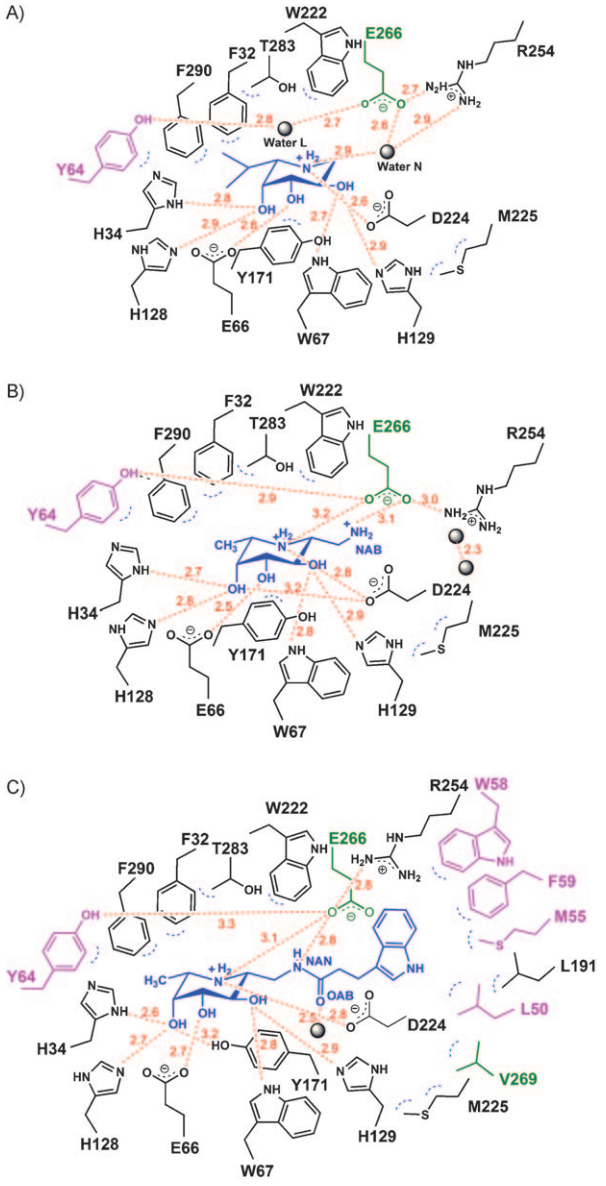

Figure 2. The inhibitor binding sites of TmF complexed with inhibitors A) **9**, B) **1**, and C) **2**. Inhibitors are shown in blue, and water molecules are shown as gray spheres. The residues of loops 1 and 2 are colored pink and dark green, respectively. Hydrogen bonds are depicted as red dashed lines with distances given in Å. Hydrophobic interactions are represented as blue dashed curves.

The positive charge of the endocyclic nitrogen (N5) elicits stronger binding than the non-charged fucose. It resembles the charged nature of the transition state. The interaction of E266 with N5 of compound **9** occurs with a water-mediated hydrogen bond, whereas there is a direct electrostatic interaction between the OE1 atom of E266 and N5 of **1**, with a distance of 3.2 Å (Figure 2A versus 2B). In addition, the OE2 atom of E266 reveals a 3.1 Å electrostatic interaction with nitrogen (NAB) of the aglycon group of compound **1** (Figure 2B). Likewise, D224 is hydrogen bonded with the O1 atom of fucose (2.7 Å;[14] Figure S5 in the Supporting Information), whereas it forms an electrostatic interaction with N5 of both compounds **1** and **9** with distances of 2.8 and 2.6 Å, respectively (Figures 2A and B, and Table S2 in the Supporting Information). Therefore, all these factors explain the relative stronger binding observed for compound **1**. This is reminiscent of the case of complexes of Cex from *Cellulomonas fimi* with xylobiose-derived azasugar inhibitors[16] and the binding of xylobiose-derived isofagomine to xylanase.[17] The result is also consistent with the studies reported by Schramm and co-workers, that transition-state analogues bind with extraordinarily high affinity relative to substrates.[18] Furthermore, D224 forms an additional hydrogen bond with the O4 atom of compound **1**. Overall, there are six hydrogen bonds between TmF and compound **9**, whereas there are nine hydrogen bonds between TmF and compound **1** (Figure 2A versus 2B). These differences explain the order of binding affinity of **1** > **9** > fucose.

Loops 1 and 2 of the TmF–**2** complex remain in the same conformation as those of the TmF–**1** complex, indicating the critical role of the endocyclic and exocyclic nitrogen atoms. However, there is still a difference in bond distances between compounds **1** and **2** with E266 of loop 2. In TmF–**2**, an electrostatic interaction and a hydrogen bond are formed between E266 and N5 and NAN, respectively. In contrast, E266 forms electrostatic interactions with N5 and NAB of compound **1** (Figure 2B versus 2C). Clearly, the distances are shorter between E266 and compound **2** than E266 and compound **1**, thereby explaining the higher binding affinity of

compound **2** toward TmF than that of **1**. In addition, the larger aglycon in compound **2** appears to greatly enhance binding affinity by increasing hydrophobic interactions, blocking the entrance of the active site groove, and removing water from the binding area. For example, compound **2** forms multiple hydrophobic interactions with L50, M55, W58, F59, L191, and V269 in loops 1 and 2 (Figure 2C). If the binding channel in the Tm–inhibitor complex is closed by the two loops and aglycon, the entrance is more hindered in the TmF–**2** complex than in the TmF–**1** and TmF–**9** complexes (Figure S3 A–C in the Supporting Information). The vital contribution of these hydrophobic interactions to tight binding is illustrated by the fact that compounds **1** and **2** both form nine hydrogen bonds with TmF (Figures 2B and C), but give very different binding affinities ($K_i = 16$ nM versus $K_i^* = 0.47$ pM). Meanwhile, the active site water molecules are ordered differently upon formation of various complex structures, as shown in Figure 2. There are three water molecules in the active site of the TmF–**9** complex, two in TmF–**1**, and only one in TmF–**2**. The observed trend supports the idea that coordination of fewer or no water molecules contributes to larger favorable entropy and tighter binding. This is consistent with the data from isothermal titration calorimetry (ITC) experiments, which indicate that $T\Delta S$ for compound **2** is greater than that of **1** (Table 1). This result is also evident in the studies reported by

Table 1: Binding constants for **1** and **2** with TmF derived by kinetic and thermodynamic methods at pH 7.5, along with the thermodynamic parameters measured with ITC.

	1	**2**
K_d	16.3 ± 2.5 nM	0.469 ± 0.14 pM
ΔG[a] [kcal mol^{-1}]	−10.7	−16.9
ΔH[b] [kcal mol^{-1}]	−2.48 ± 0.28	−6.23 ± 0.22
$T\Delta S$[c] [kcal mol^{-1}]	8.22	10.69

[a] ΔG values were calculated from the inhibition constants using the equation $\Delta G = RT\ln K_d$. [b] ΔH values were determined from ITC titrations of a single subunit on the enzyme. [c] The Gibbs free energy equation was used to calculate $-T\Delta S$.

the research groups of Davies and Schramm.[19,20] However, Jencks raised a concern about the interpretation in entropies, and listed several other possible factors that provide favorable binding energies.[21]

The pH dependence of inhibition supports the protonation of the endocyclic nitrogen atom. The catalytic profile for TmF is bell-shaped, with an optimum at pH 5.0 and respective acidic and basic limbs of pK_a 3.6 and 6.7, suggesting titration of the catalytic nucleophile and acid/base, respectively (Figure 3).[5] The pH dependence of $1/K_i$ for **2** gives acidic and basic limbs of pK_a 5.3 and 7.2, respectively. The alkaline shift of the acid leg simply reveals that a protonated inhibitor cannot bind tightly due to protonation of the acid/base. Elsewhere this alkaline shift in pH dependence has been interpreted as a protonated inhibitor optimally

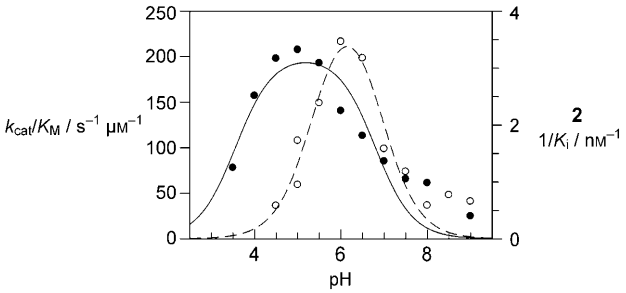

Figure 3. pH dependence of k_{cat}/K_M for TmF (●) and $1/K_i$ for **2** (○). Fits to bell-shaped profiles are shown for k_{cat}/K_M (——) and $1/K_i$ for **2** (-----). The fitted curves were generated with the GraFit software package.

binding to an enzyme, the acid/base and nucleophile of which are both ionized.[5]

The flexibility of aglycon affects the compactness of the enzyme–inhibitor complex. For instance, there are two methylene units between the indole group and amide of compound **2**, which fits snugly in the binding site to block the entire entrance. In contrast, the aglycon of compound **4** (or **6**), which lacks such methylene groups, is restricted by its own rigidity so that it packs loosely and only partially obstructs the entrance (Figure 4 and Figure S2 in the Supporting Information). This structural difference accounts for the 100-fold difference in inhibition potency. An inhibitor with two flexible hydrophobic substituents might improve the K_i value to the femtomolar range if they interact with the two loops simultaneously. The interaction between the two loops and the C1 aglycon is linked to the stability of the loop closure, which is consistent with our previous finding that the introduction of C1 aglycon is indispensable for the occurrence of slow-binding inhibition.[12,13] The stable extent of the closed conformation likely explains why compound **2** is the most potent inhibitor with the highest K_i/K_i^* ratio (224) as compared with compounds **3**–**7**, which have K_i/K_i^* ratios ranging from 2 to 19 (Figure 1).[22] Loops are often invisible in X-ray crystal structures owing to their flexibility. Loops near the enzyme active site can be a consideration during drug design if their conformation stabilizes upon binding with small molecules. For example, the active site of HIV-1 protease is gated by two extended β hairpin loops, also known as flaps.[23] Flap flexibility is essential for catalysis,[24]

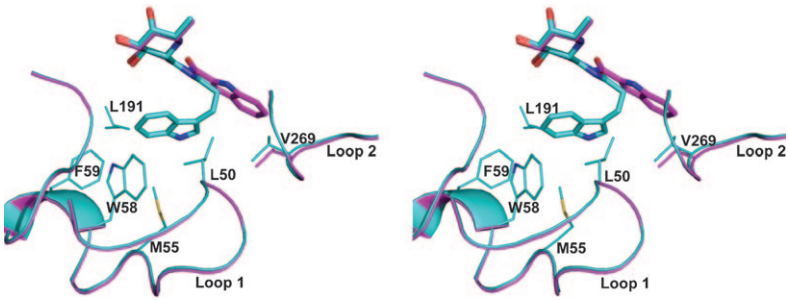

Figure 4. Comparison of the inhibitor binding sites of TmF complexed with inhibitors **2** (cyan) and **4** (magenta) is presented in stereo view; loops 1 and 2 are indicated.

and targeting flap movement has been an effective approach in the development of HIV protease inhibitors.

TmF is the closest bacterial relative of mammalian α-fucosidases.[14] Interestingly, sequence alignment reveals striking differences between TmF and *Homo sapiens* α-fucosidase (HuF) in loops 1 and 2. Loop 1 is completely missing in HuF, and loop 2 in HuF is shorter than that of TmF (Figure S6 in the Supporting Information). Consequently, FNJ derivatives with a more rigid aglycon at the C1 position would probably inhibit HuF activity more effectively by directly blocking the substrate binding tunnel. This hypothesis has been corroborated by inhibition screening with our "in-house" library. The best inhibition is observed with compound **1** ($K_i = 15.2$ nM for HuF) coupled to 9-fluorene-1-carboxylic acid.[12,13] The product **10** has a K_i value of 0.40 nM, implying a 38-fold improvement in binding affinity (Figure 1).[25]

In conclusion, the analysis of these enzyme–inhibitor complex structures demonstrates how the enzyme interacts with various inhibitors to span a 10^6-fold range in potency and identifies the important factors for improving the binding affinity and inhibition potency. The level of low micromolar affinity provides sufficient binding interactions for the stabilization of loops 1 and 2, in the main control of Y64, D224, and E266. The two loops do not just provide hydrogen bonds and electrostatic interactions, but further improvement of K_i values from nanomolar to picomolar is also contributed by increases in hydrophobic interactions and in entropy. Additionally, the flexibility of aglycon and the resulting hydrophobic/hydrogen-bond interactions likely further fine-tune the K_i value in the picomolar range. These results clearly provide valuable insight in the design of potent enzyme inhibitors.

Received: October 7, 2009
Revised: November 5, 2009
Published online: December 3, 2009

Keywords: fucosidases · iminocyclitols · inhibitors · slow binding

[1] N. Asano, *Glycobiology* **2003**, *13*, 93R – 104R.
[2] W. Lew, X. Chen, C. U. Kim, *Curr. Med. Chem.* **2000**, *7*, 663 – 672.
[3] A. Mitrakou, N. Tountas, A. E. Raptis, R. J. Bauer, H. Schulz, S. A. Raptis, *Diabetic Med.* **1998**, *15*, 657 – 660.
[4] S. G. Withers, M. Namchuk, R. Mosi in *Iminosugars as Glucosidase Inhibitors: Nojirimycin and Beyond* (Ed.: A. E. Stutz), Wiley-VCH, Weinheim, **1999**, pp. 188 – 206.
[5] a) A. Varrot, C. A. Tarling, J. M. Macdonald, R. V. Stick, D. L. Zechel, S. G. Withers, G. J. Davies, *J. Am. Chem. Soc.* **2003**, *125*, 7496 – 7497; b) Y. W. Kim, A. L. Lovering, H. Chen, T. Kantner, L. P. McIntosh, N. C. Strynadka, S. G. Withers, *J. Am. Chem. Soc.* **2006**, *128*, 2202 – 2203; c) T. M. Gloster, P. Meloncelli, R. V. Stick, D. Zechel, A. Vasella, G. J. Davies, *J. Am. Chem. Soc.* **2007**, *129*, 2345 – 2354; d) M. E. Caines, S. M. Hancock, C. A. Tarling, T. M. Wrodnigg, R. V. Stick, A. E. Stutz, A. Vasella, S. G. Withers, N. C. Strynadka, *Angew. Chem.* **2007**, *119*, 4558 – 4560; *Angew. Chem. Int. Ed.* **2007**, *46*, 4474 – 4476; e) D. A. Kuntz, C. A. Tarling, S. G. Withers, D. R. Rose, *Biochemistry* **2008**, *47*, 10058 – 10068.
[6] L. V. Hooper, J. I. Gordon, *Glycobiology* **2001**, *11*, 1R – 10R.
[7] D. Ayude, J. Fernandez-Rodriguez, F. J. Rodriguez-Berrocal, V. S. Martinez-Zorzano, A. de Carlos, E. Gil, M. Paez de La Cadena, *Oncology* **2000**, *59*, 310 – 316.
[8] M. C. Glick, V. A. Kothari, A. Liu, L. I. Stoykova, T. F. Scanlin, *Biochimie* **2001**, *83*, 743 – 747.
[9] P. J. Willems, R. Gatti, J. K. Darby, G. Romeo, P. Durand, J. E. Dumon, J. S. O'Brien, *Am. J. Med. Genet.* **1991**, *38*, 111 – 131.
[10] W. L. Hutchinson, P. J. Johnson, M. Q. Du, R. Williams, *Clin. Sci.* **1991**, *81*, 177 – 182.
[11] T. W. Liu, C. W. Ho, H. H. Huang, S. M. Chang, S. D. Popat, Y. T. Wang, M. S. Wu, Y. J. Chen, C. H. Lin, *Proc. Natl. Acad. Sci. USA* **2009**, *106*, 14581 – 14586.
[12] C. W. Ho, Y. N. Lin, C. F. Chang, S. T. Li, Y. T. Wu, C. Y. Wu, C. F. Chang, S. W. Liu, Y. K. Li, C. H. Lin, *Biochemistry* **2006**, *45*, 5695 – 5702.
[13] C. F. Chang, C. W. Ho, C. Y. Wu, T. A. Chao, C. H. Wong, C. H. Lin, *Chem. Biol.* **2004**, *11*, 1301 – 1306.
[14] G. Sulzenbacher, C. Bignon, T. Nishimura, C. A. Tarling, S. G. Withers, B. Henrissat, Y. Bourne, *J. Biol. Chem.* **2004**, *279*, 13119 – 13128.
[15] G. Davis, M. L. Sinnott, S. G. Withers in *Comprehensive Biological Catalysis* (Ed.: M. L. Sinnott), Academic Press, London, **1997**, pp. 119 – 209.
[16] V. Notenboom, S. J. Williams, R. Hoos, S. G. Withers, D. R. Rose, *Biochemistry* **2000**, *39*, 11553 – 11563.
[17] T. M. Gloster, S. J. Williams, S. Roberts, C. A. Tarling, J. Wicki, S. G. Withers, G. J. Davies, *Chem. Commun.* **2004**, 1794 – 1795.
[18] a) V. Singh, G. B. Evans, D. H. Lenz, J. M. Mason, K. Clinch, S. Mee, G. F. Painter, P. C. Tyler, R. H. Furneaux, J. E. Lee, P. L. Howell, V. L. Schramm, *J. Biol. Chem.* **2005**, *280*, 18265 – 18273; b) Y. Zhang, M. Luo; V. L. Schramm, *J. Am. Chem. Soc.* **2009**, *131*, 4685 – 4694; V. L. Schramm, *J. Am. Chem. Soc.* **2009**, *131*, 4685 – 4694.
[19] T. M. Gloster, S. Roberts, G. Perugino, M. Rossi, M. Moracci, N. Panday, M. Terinek, A. Vasella, G. J. Davies, *Biochemistry* **2006**, *45*, 11879 – 11884.
[20] A. A. Edwards, J. M. Mason, K. Clinch, P. C. Tyler, G. B. Evans, V. L. Schramm, *Biochemistry* **2009**, *48*, 5226 – 5238.
[21] a) W. P. Jencks, *Adv. Enzymol. Relat. Areas Mol. Biol.* **1975**, *43*, 219 – 410. In addition, relatively minor changes in ligands or conditions also cause alteration in the binding entropy. See: b) A. K. Samland, I. Jelesarov, R. Kuhn, N. Amrhein, P. Macheroux, *Biochemistry* **2001**, *40*, 9950 – 9956; c) C. K. Huang, P. Wei, K. Q. Fan, Y. Liu, L. H. Lai, *Biochemistry* **2004**, *43*, 4568 – 4574.
[22] A. L. Perryman, J. H. Lin, J. A. McCammon, *Biopolymers* **2006**, *82*, 272 – 284.
[23] N. E. Kohl, E. A. Emini, W. A. Schleif, L. J. Davis, J. C. Heimbach, R. A. Dixon, E. M. Scolnick, I. S. Sigal, *Proc. Natl. Acad. Sci. USA* **1988**, *85*, 4686 – 4690.
[24] L. K. Nicholson, T. Yamazaki, D. A. Torchia, S. Grzesiek, A. Bax, S. J. Stahl, J. D. Kaufman, P. T. Wingfield, P. Y. Lam, P. K. Jadhav, C. N. Hodge, P. J. Domaille C.-H. Chang, *Nat. Struct. Biol.* **1995**, *2*, 274 – 280.
[25] We also tested compounds **2**, **4**, **5**, and **6** against human fucosidase, and their respective K_i values are: (5.6 ± 0.2), (33.8 ± 2.8), (18.0 ± 0.2), and (53.8 ± 0.9) nM.

